

Relationship between median destructive field and remanent coercive forces for dispersed natural magnetite, titanomagnetite and hematite

Peter Dankers *Paleomagnetisch Laboratorium 'Fort Hoofddijk', Budapestlaan 17, Utrecht, The Netherlands*

Received 1980 April 28; in original form 1979 October 16

Summary. Remanent acquisition curves, remanent hysteresis curves and alternating field demagnetization curves were determined for a number of artificial rock specimens containing well-defined grain-size fractions between 5 and 250 μm of natural magnetite, titanomagnetite and hematite. From these curves, the remanent acquisition coercive force H'_{cr} , the remanent coercive force H_{cr} and the median destructive field of IRM $H_{1/2\text{I}}$ were determined. Theoretically these parameters should be the same for an assembly of non-interacting, homogeneously distributed, randomly oriented single-domain grains. For a given hematite specimen H'_{cr} , H_{cr} and $H_{1/2\text{I}}$ have about the same value in spite of the strong grain-size dependence of these parameters. For each specimen of magnetite and titanomagnetite the value of H'_{cr} is larger than H_{cr} which again is larger than $H_{1/2\text{I}}$. However, the ratios $H'_{\text{cr}}/H_{\text{cr}}$ and $H_{1/2\text{I}}/H_{\text{cr}}$ appear to have a (different) constant value. An interesting relationship which appears to hold for dispersed magnetite, titanomagnetite or hematite grains between 5 and 250 μm , independently of grain-size, quantity and packing density of the magnetic material, is:

$$H'_{\text{cr}} + H_{1/2\text{I}} \approx 2H_{\text{cr}}.$$

Introduction

In rock magnetic and palaeomagnetic research, the remanent coercive force H_{cr} , and the median destructive field $H_{1/2}$ are frequently used to characterize the stability of the carriers of remanent magnetization of rock specimens. Both parameters are an expression of the coercivity which is the ability of a magnetization of magnetic material to resist reorienting forces. The remanent coercive force is the direct magnetic field strength required to reorient one-half of the remanent saturation magnetization in the opposite direction. In this study the median destructive field of the remanent saturation magnetization ($H_{1/2\text{I}}$) will be used. It is defined as the strength of the alternating magnetic field required to eliminate one-half of the remanent saturation magnetization. An expression for coercivity which is less used is

Present address: Earth Physics Branch, Energy, Mines and Resources, 1 Observatory Crescent, Ottawa, Ontario K1A 0Y3, Canada.

the remanent acquisition coercive force H'_{cr} , defined as the magnetic field strength required to magnetize a not previously magnetized magnetic material to one-half of its remanent saturation magnetization.

All the parameters mentioned above yield some information about coercivity. However, the relationship between them is not very well established; the reason being that each parameter is a function of many interdependent properties of the magnetic material. For an assembly of magnetic grains such properties include the domain configuration, the demagnetizing factor N , the magnetic moment, the grain size, the interaction between grains and the distribution of the grains. According to Wohlfarth (1958), for an assembly of homogeneously distributed, randomly oriented, uniaxial non-interacting single-domain grains, H'_{cr} , H_{cr} and $H_{1/2I}$ will all have the same value. However, these conditions are rarely observed in natural rocks. Dunlop & West (1969) have shown that interaction between dispersed single-domain grains of magnetite does occur and has a significant effect on the coercivity. The grain-size dependence of H_{cr} for dispersed magnetite grains has been studied by Parry (1965) who found an increase of H_{cr} with decreasing grain size for assemblies of grains ranging in size from 120 to 6 μm . The coercivity of acicular single-domain grains is larger than that of equidimensional grains of similar size.

All the above-mentioned parameters have to be taken into account while studying the relationship between H'_{cr} , H_{cr} and $H_{1/2I}$. In this study particular attention is given to the effects of grain size, packing density and related grain interaction. To avoid complications, all other properties have to be kept the same. Hence, a series of artificial specimens were made by dispersing homogeneously magnetic grains of constant shape but different size and random orientation in a non-magnetic matrix. The effect of grain-interaction on H'_{cr} , H_{cr} and $H_{1/2I}$ and their relationship was studied by preparing specimens having the same grain-size fraction but different packing densities of the magnetic grains.

Preparation of the specimens

Artificial specimens of dispersed magnetic grains were prepared by mixing known quantities of well-determined grain-size fractions of natural magnetic minerals with aluminium oxide powder and waterglass ($\text{Na}_2\text{O} \times \text{SiO}_2$). The magnetic minerals used in this study are: two magnetities, one titanomagnetite and three different types of hematite. These minerals were obtained by separating them from crushed rocks or ores using heavy liquids in a liquid overflow centrifuge (IJst 1973) and by magnetic separation using a Frantz isodynamic separator which is adapted for separating fine, strongly magnetic grains (Green & Cornitius 1971). The magnetic separates were sieved ultrasonically in acetone with photo-etched micro-precision-sieves, having circular hole-diameters of respectively 5, 10, 15, 20, 25, 30, 40, 55, 75, 100, 150 and 250 μm . Each grain-size fraction was examined optically for impurities and for uniformity of grain size. If necessary a fraction was sieved and separated once more to ensure high purity (> 95 per cent) and uniform grain size. Much care was taken to prevent oxidation of the magnetite and titanomagnetite grains during the separation procedure. Therefore, crushing of the rocks was done under a nitrogen atmosphere and ultrasonic sieving and magnetic separation in acetone.

Electron microprobe analysis and X-ray diffraction was performed on one separated grain-size fraction of each sample (Table 1). A more detailed description of the samples is given by Dankers (1978).

In order to be able to verify theoretical models, precautions were taken to disperse the magnetic grains homogeneously and randomly in the non-magnetic matrix. Therefore the aluminium oxide powder was first poured into a perspex cylinder and then the magnetic

Table 1. Composition of the samples.

Sample number	MgO	Al ₂ O ₃	SiO ₂	TiO ₂	Cr ₂ O ₃	MnO	FeO	Fe ₂ O ₃	Lattice parameters	Shape of the grains
LM 1	—	0.12	0.35	0.10	—	—	31.03	68.91	8.399 ± 0.005	Equidimensional magnetite
LM 3	—	—	0.29	—	—	—	30.90	68.75	8.400 ± 0.004	Equidimensional magnetite
DLA	2.75	1.56	0.44	26.67	0.12	0.66	51.59	15.57	8.476 ± 0.008	Equidimensional titanomagnetite
LH1	—	—	1.02	—	—	—	—	96.92	5.050 ± 0.012	Platy hematite
LH2	—	0.10	0.41	—	—	—	—	98.18	13.75 ± 0.04	Platy hematite
LH3	—	0.32	0.42	—	—	—	—	98.22	13.75 ± 0.04	Platy hematite

fraction was added, the mixture being stirred thoroughly. Lastly, the waterglass, a viscous liquid, was added little by little under intensive stirring until a compact mass was obtained. The mass was moulded in a perspex cylinder of 2.5 cm diameter and 2.2 cm height which is the size and shape of rock specimens normally used in palaeomagnetic research. The specimens were allowed to harden for several weeks in a zero field.

Mass and packing density of the magnetic grains

As we wish to investigate the effect of packing density on the interacting field, it is important to establish both the number of grains per unit volume and the volume percentage magnetic material in each specimen.

The volume of all specimens is about 10 cm^3 . If in this volume the same mass of a different grain-size fraction is dispersed, the packing density of the magnetic grains will be different because a smaller number of coarse grains will have the same weight as a larger number of fine grains. By measuring the dimensions of a number of grains of each grain-size fraction and calculating the mean grain volume of each, an estimate can be made of the number of magnetic grains per unit volume in a specimen.

By making specimens with different quantities of the same grain-size fraction, the effect of packing density can be examined for a given grain size. To bring the investigation within manageable limits, specimens with different packing densities but the same grain-size fraction were made from only six magnetite fractions, and one titanomagnetite fraction. From all other grain-size fractions of magnetite a quantity of about 0.25 g was used which resulted in specimens that could be measured easily with the apparatus available. For most of the titanomagnetite specimens a mass of 0.1 g was used because only a little material was available. Because hematite has a small spontaneous magnetization, 0.5 g of each grain-size fraction was used to obtain specimens that could be measured easily. Problems arose for highly diluted specimens owing to the slightly magnetic character of the aluminium oxide powder; for these specimens corrections had to be made. This was done by measuring remanent acquisition curves, remanent hysteresis curves and alternating field demagnetization curves of 10 blank specimens. The average intensities obtained from the blank runs were subtracted from the corresponding points of the intensity-curves of the diluted specimens.

Experimental procedure

After the specimens were prepared and stored in a zero field to harden, the residual remanent magnetizations were usually less than 1 per cent of the remanent saturation magnetization. Subsequently the specimens were magnetized in a stepwise manner up to 20 kOe. (For technical reasons CGS units are used in this paper. $1 \text{ Oe} = 0.1 \text{ mT}$, $1 \text{ emu} = 10^{-3} \text{ Am}^2$, $1 \text{ (emu/g)} = 1 \text{ (Am}^2/\text{kg)}$.) After each magnetization step, the remanent magnetization was measured using four flux gates, arranged non-inductively in Helmholtz coils. Both the remanent saturation magnetization per gram magnetic material (M_{sr}) and the remanent acquisition coercive force (H'_{cr}) could be derived from the remanent acquisition curve thus obtained. After reaching the maximal field, the specimen was placed oppositely to the previous orientation between the pole-shoes of the electromagnet. Again the specimen was stepwise magnetized until remanent saturation magnetization was reached in the opposite direction. The last procedure was repeated. Hence, for each specimen the remanent coercive force was measured twice and the remanent saturation magnetization three times.

After the last magnetization step in a direct field of 20 kOe, the specimens were stepwise demagnetized with alternating magnetic fields up to 3000 Oe. At each alternating field

strength the specimen was demagnetized along the three orthogonal axes and the remanent magnetization was measured with an astatic magnetometer. If necessary, the values were corrected for the aluminum oxide matrix and the median destructive field ($H_{1/2I}$) was determined from the corrected decay curves.

The reproducibility of the measurements appeared to be very good. The standard error for M_{sr} , calculated from the three measurements carried out for each specimen, was smaller than 0.5 per cent for all specimens. The standard error for H_{cr} , calculated from two measurements for each specimen, usually did not exceed 5 Oe for magnetite and titanomagnetite and was 1 to 2 per cent for hematite. For H'_{cr} and $H_{1/2I}$ no standard error could be determined because only one measurement of these parameters was done per specimen. However, because the errors are mainly determined by the technique used, it is expected that the standard error for H'_{cr} will be the same as for H_{cr} . An estimate of the standard error for $H_{1/2I}$, based on the scatter of the measuring points of the alternating field demagnetization curves, reveals values of less than 5 Oe for magnetite and titanomagnetite and 2 per cent for hematite.

Results and their interpretation

HEMATITE

The artificial hematite specimens used in this study fulfil the requirements for being assemblies of homogeneously distributed and randomly oriented, non-interacting single-domain grains. It is unlikely that interaction between hematite grains occurs at room temperature because of their low magnetic moment, at this temperature. Grains of hematite are expected to be single domain up to a size of some tens of microns.

High direct magnetic fields are required to reach remanent saturation magnetization (I_{sr}) for hematite. For fine grains of hematite, the maximal available field of 20 kOe was not quite enough to reach saturation remanence. The range of the remanent saturation magnetization per gram magnetic material (M_{sr}) for hematite specimens is not very large (Table 2, Fig. 1), although fine grains have higher M_{sr} values than coarse grains. There is also very little difference of M_{sr} between the different hematite samples. This is in contrast to grain-size dependence of H_{cr} which varies greatly for the various hematite samples (Table 3, Fig. 1).

H_{cr} values of sample LH 2 are surprisingly low (600 Oe and less) whereas sample LH 1 and sample LH 3 have higher values. The lower coercivity of LH 2 is consistent with its much larger anisotropic magnetic moment, determined by cooling the specimens to temperatures below the Morin transition (Dankers 1978). One characteristic of the hematite samples

Table 2. Mass magnetic material and remanent saturation magnetization per gram magnetic material (M_{sr}) for hematites.

Grain-size μm	LH 1		LH 2		LH 3	
	Weight gr	M_{sr} $\frac{\text{emu}}{\text{gr}}$	Weight gr	M_{sr} $\frac{\text{emu}}{\text{gr}}$	Weight gr	M_{sr} $\frac{\text{emu}}{\text{gr}}$
150 - 250	0.50	0.219	0.28	0.215	0.50	0.186
100 - 150	0.50	0.219	0.54	0.219	0.50	0.190
75 - 100	0.50	0.213	0.50	0.224	0.50	0.190
55 - 75	0.50	0.220	0.52	0.218	0.50	0.194
40 - 55	0.50	0.223	0.50	0.219	0.50	0.197
30 - 40	0.50	0.218	0.56	0.224	0.50	0.200
25 - 30	0.50	0.240	0.50	0.234	0.50	0.200
20 - 25	0.50	0.239	0.50	0.240	0.50	0.200
15 - 20	0.47	0.220	0.36	0.251	0.28	0.236
10 - 15	0.50	0.240	0.50	0.231	0.50	0.199
5 - 10	0.47	0.254			0.50	0.222
< 5	0.50	0.263			0.50	0.204

Table 3. Remanent acquisition coercive force H'_{cr} , remanent coercive force H_{cr} and median destructive field $H_{1/2I}$ of hematites. All values are given in oersted.

Grain-size μm	LH 1			LH 2			LH 3		
	H'_{cr}	H_{cr}	$H_{1/2I}$	H'_{cr}	H_{cr}	$H_{1/2I}$	H'_{cr}	H_{cr}	$H_{1/2I}$
150 - 250	2510	2930	-	550	590	530	2900	3050	2730
100 - 150	1780	2150	-	530	550	580	2750	2800	-
75 - 100	2450	2900	-	550	600	580	2300	2415	2340
55 - 75	2430	2750	-	350	590	580	1310	1430	1745
40 - 55	-	-	-	570	610	640	1710	1730	1970
30 - 40	-	2830	-	650	700	735	1550	1660	1865
25 - 30	2450	2725	-	650	725	825	2250	2290	-
20 - 25	2680	2990	-	775	875	860	2510	2580	2360
15 - 20	2750	3150	-	960	1000	1180	2600	2750	2850
10 - 15	3050	3480	-	1350	1400	1270	2800	3000	2735
5 - 10	3530	3800	-	-	-	-	3160	3050	-
< 5	4000	4100	-	-	-	-	3360	4475	-

$H_{1/2I}$ of specimens of LH 1 and some specimens of LH 3 could not be determined (-) because they exceeded 3000 Oe, the maximum alternating magnetic field available. Weight quantity magnetic material is the same as in Table 2.

is that for grains finer than about 30 μm , H_{cr} increases with decreasing grain size whereas above 30 μm there is hardly any grain-size dependence of H_{cr} except for LH 3 where, for grain sizes greater than 30 μm , H_{cr} increases with grain size. The abrupt change in slope in the curves might reflect differences in domain configuration, where hematite grains finer than 30 μm are single-domain (sd) whereas coarser grains might be pseudo-single-domain (psd) or multi-domain (md). Since internal stress appears to play an important role in the coercivity of fine grained hematite (Stacey & Banerjee 1974, p. 86), it is also possible that the change in slope is caused by increased internal stress of fine grains with respect to coarse grains.

The remanent acquisition curves of each hematite specimen lie completely within the remanent hysteresis curves (Fig. 2). The value of H'_{cr} is always lower than the value of H_{cr} for the same specimen (Table 3). The relationship between H'_{cr} and H_{cr} is shown in

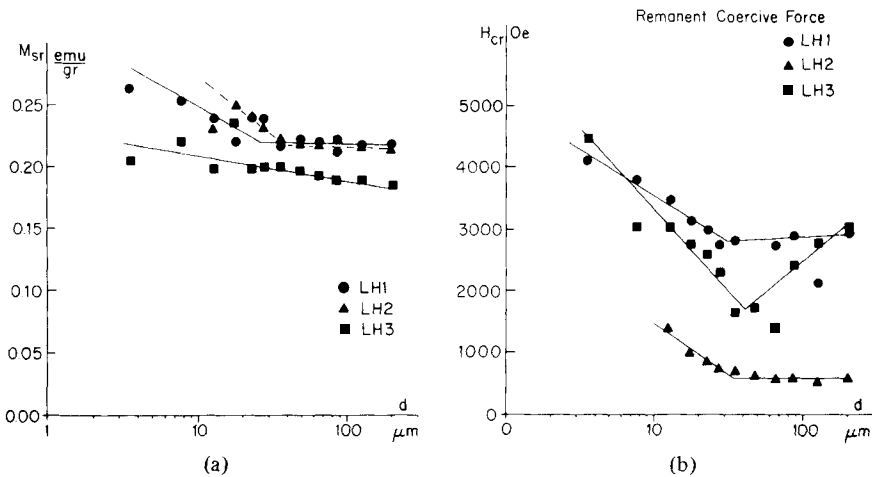


Figure 1. (a) Remanent saturation magnetization per gram magnetic material (M_{sr}) and (b) remanent coercive force (H_{cr}) for different grain-size fractions of hematite samples LH 1, LH 2, LH 3. The maximum direct magnetic field used to magnetize the specimens was 20 kOe. For most of the specimens this field strength was strong enough to achieve saturation remanence. The marked change in slope for H_{cr} at a grain-size of about 30 μm might reflect the transition from single-domain to multi-domain configuration.

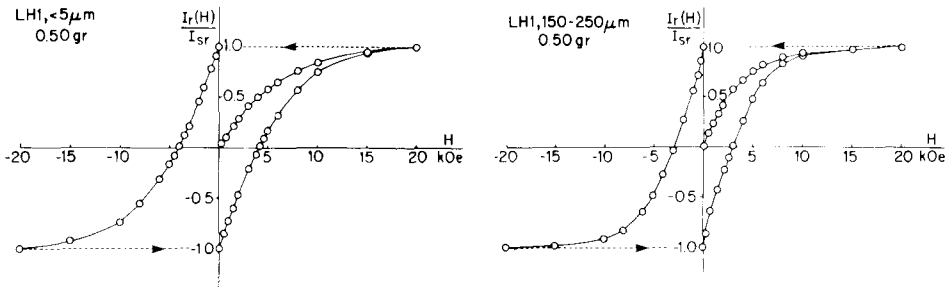


Figure 2. Normalized remanent acquisition curves and normalized remanent hysteresis curves for a fine-grained and a coarse-grained fraction of the same hematite sample. The remanent acquisition curves lie completely within the remanent hysteresis curves. For both specimens the remanent acquisition coercive force H'_{cr} has about the same strength as the remanent coercive force H_{cr} . I_{sr} is the remanent saturation magnetization and $I_r(H)$ is the remanent magnetization after applying a direct magnetic field H .

Fig. 3. Results of LH 2 and LH 3 plot on the same line with a slope of $44^\circ \pm 3^\circ$ through the origin. Results for LH 1 give a line that is parallel with, but offset from, the lines of LH 2 and LH 3. The offset may be the result of not quite reaching saturation remanence.

Alternating field demagnetization in 3000 Oe of the remanent saturation magnetization of all specimens of LH 1 and the finest grain size specimens of LH 3 was insufficient to reduce the intensity to one-half of its original value. Therefore the $H_{\frac{1}{2}I}$ could not be determined for these specimens. The $H_{\frac{1}{2}I}$ s that could be determined were strikingly similar to the values of H_{cr} of the same specimen (Table 3, Fig. 4). The best-fitting line through the points giving the relationship between H_{cr} and $H_{\frac{1}{2}I}$ for LH 2 and LH 3 has a slope of $45^\circ \pm 5^\circ$. Again, it appears that the results for LH 1 would be on a different line since $H_{\frac{1}{2}I}$ is at least 3000 Oe for all specimens of LH 1 whereas some of the values of H_{cr} are lower than 3000 Oe (Table 3).

From these results it can be concluded that for dispersed hematite grains ranging in size from 5 to 250 μm , the relationships between H'_{cr} and H_{cr} and between $H_{\frac{1}{2}I}$ and H_{cr} are

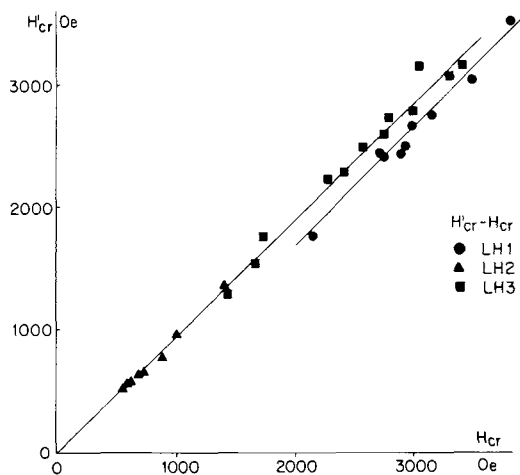


Figure 3. Relationship between the remanent acquisition coercive force (H'_{cr}) and the remanent coercive force (H_{cr}) for various grain-size fractions of hematite samples LH 1, LH 2 and LH 3. The slope of the lines is $44^\circ \pm 3^\circ$. The offset of the line for LH 1 might be due to incomplete remanence saturation.

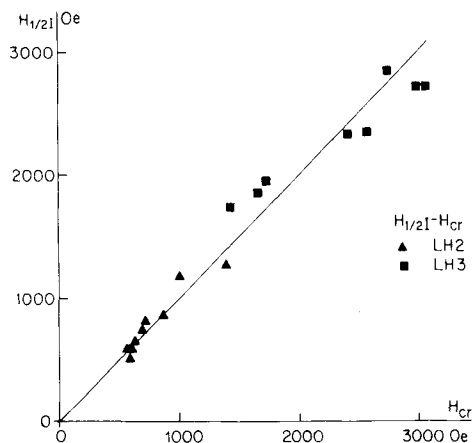


Figure 4. Relationship between the median destructive field of the remanent saturation magnetization ($H_{1/2I}$) and the remanent coercive force (H_{Cr}) for various grain-size fractions of hematite samples LH 2 and LH 3. The slope of the line is $45^\circ \pm 5^\circ$. No results for sample LH 1 can be given because $H_{1/2I}$ of all specimens of LH 1 is higher than 3000 Oe, the maximum alternating magnetic field available.

independent of grain size of the magnetic grains. Both ratios are close to unity which means that for homogeneously distributed and randomly oriented hematite grains $H'_{Cr} = H_{Cr} = H_{1/2I}$.

MAGNETITE AND TITANOMAGNETITE

Magnetite has a high magnetic moment and a low coercivity which means that grain interactions and self-demagnetization effects may play an important role in determining the magnetic properties of an assembly of magnetite grains.

A theoretical model for interacting single-domain grains was proposed by Dunlop & West (1969) who modified Néel's (1955) theory by introducing the assumption that the interacting field can be treated as though it were independent of the external field. They concluded that the effective coercivity of a particle during alternating field demagnetization is always lowered by grain interactions. Levi & Merrill (1978) found that for equidimensional submicron magnetic particles H_{Cr} and $H_{1/2I}$ are mainly determined by shape anisotropy and that packing of grains is not very important. According to the results of Day, Fuller & Schmidt (1977) for magnetite, concentrations of greater than 5 per cent by weight are required before packing density will begin decreasing H_{Cr} . For titanomagnetites with high Ti-values they could not establish a dependence of coercivity versus concentration.

The domain configuration of the magnetite grains used in this study ranges from psd to md. The transition to truly md grains of magnetite is about 10–20 μm (Day *et al.* 1977). The transition size increases with increasing Ti-content and will be about 30–40 μm for titanomagnetite with $x = 0.6$ (Day *et al.* 1977). Titanomagnetite used in this study will therefore be mainly psd.

For all specimens of magnetite and titanomagnetite, remanent saturation magnetization was achieved in direct magnetic fields well below 20 kOe. The intensity of the remanent saturation magnetization per gram of magnetic material (M_{sr}) is very strongly dependent upon grain size for magnetite and to a lesser extent for titanomagnetite (Table 4, Fig. 5). The total remanent saturation magnetization I_{sr} for diluted specimens of a certain grain-size fraction is, of course, much less than for specimens containing more material. The specific remanent saturation magnetization M_{sr} , however, is mainly determined by the size of the

Table 4. Mass magnetic material and remanent saturation magnetization per gram magnetic material (M_{sr}) of magnetites and titanomagnetites.

Grain-size μm	LM 1		LM 3		DLA	
	Weight	M_{sr}	Weight	M_{sr}	Weight	M_{sr}
	gr	$\frac{\text{emu}}{\text{gr}}$	gr	$\frac{\text{emu}}{\text{gr}}$	gr	$\frac{\text{emu}}{\text{gr}}$
150 - 250	0.40	0.90	0.25	0.64		
100 - 150	0.25	0.97	0.25	0.77		
75 - 100	0.25	1.16	0.25	1.01		
55 - 75	0.25	1.11	0.25	1.32		
40 - 55	0.25	1.62	0.25	1.85		
30 - 40	0.25	1.74	0.25	1.89	0.07	0.70
25 - 30	0.25	2.31	0.25	2.57	0.10	0.84
20 - 25	0.25	3.56	0.25	3.88	0.10	1.12
15 - 20	0.25	3.86	0.25	4.69	0.10	1.28
10 - 15	0.25	5.09	0.26	5.07	0.10	1.55
5 - 10	0.27	11.07	0.22	6.53	0.10	1.74
< 5	0.25	15.06	0.25	12.24	0.10	3.00

Table 5. Remanent acquisition coercive force H'_{cr} , remanent coercive force H_{cr} and median destructive field $H_{1/2I}$ of magnetites and titanomagnetite. All values are given in oersteds.

Grain-size μm	LM 1			LM 3			DLA		
	H'_{cr}	H_{cr}	$H_{1/2I}$	H'_{cr}	H_{cr}	$H_{1/2I}$	H'_{cr}	H_{cr}	$H_{1/2I}$
150 - 250	250	160	55	270	170	65			
100 - 150	265	175	65	320	195	65			
75 - 100	295	180	65	330	200	75			
55 - 75	310	185	75	340	215	75			
40 - 55	310	190	70	350	215	80			
30 - 40	335	195	80		195	90	105	85	45
25 - 30	330	195	80		210	85	85	85	50
20 - 25	390	205	90	360	215	90	110	110	60
15 - 20	435	245	100		245	100		110	60
10 - 15	350	185	115		240	100	160	120	65
5 - 10	540	235	165		280	115	180	140	85
< 5	630	300	185	625	410	180	295	230	150

Weight quantity magnetic material is the same as in Table 4.

Table 6. Magnetic parameters for specimens containing different quantities of magnetic materials of the same grain size.

Sample	Grain-size μm	Mass gr	Volume % %	Number of Grains Volume Specimen $\times 10^4/\text{cm}^3$	M_{sr}	H'_{cr}	H_{cr}	$H_{1/2I}$
					$\frac{\text{emu}}{\text{gr}}$	Oe	Oe	Oe
LM 1	150 - 250	1.59	3.97	0.90	0.82	245	150	55
	150 - 250	0.40	0.81	0.23	0.90	250	160	55
LM 3	100 - 150	3.04	6.18	6.1	0.79	285	165	71
	100 - 150	0.25	0.51	0.50	0.77	320	195	65
LM 3	25 - 30	0.25	0.51	49.	2.57		210	85
	25 - 30	0.023	0.05	4.5	2.41	355	215	85
	25 - 30	0.0011	0.002	0.22	3.68	310	190	72
LM 1	20 - 25	0.25	0.51	91.	3.56	390	205	90
	20 - 25	0.01	0.02	3.7	2.87	390	240	
	20 - 25	0.0015	0.003	0.55	2.98	410	250	95
LM 3	15 - 20	0.25	0.51	198.	4.69		245	100
	15 - 20	0.01	0.02	7.9	3.93	415	250	102
	15 - 20	0.0009	0.002	0.72	4.55	450	265	108
LM 1	5 - 10	0.27	0.55	3050.	11.07	540	235	165
	5 - 10	0.01	0.02	112.	9.81	595	375	160
	5 - 10	0.001	0.002	11.	9.87	640	385	154
DLA	5 - 10	0.10	0.20	1195.	1.74	180	140	85
	5 - 10	0.0024	0.005	28.	1.79	190	140	72

grains and not by the quantity. Davis & Evans (1976) reported for strong concentrations of magnetite a lowering of M_{sr} which was due to interactions. In our results no such a trend was observed (Table 6) which may indicate either that the concentration of magnetite in our specimen was not strong enough so that no interaction between grains exists or that M_{sr} is only reduced slightly.

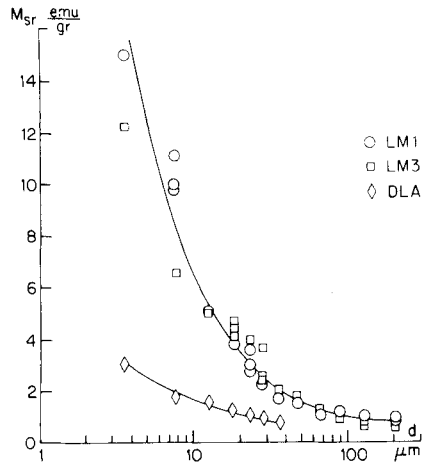


Figure 5. Remanent saturation magnetization per gram magnetic material (M_{sr}) for different grain-size fractions of magnetite, samples LM 1 and LM 3 and titanomagnetite sample DLA.

The relative position of the remanent acquisition curve with respect to the remanent hysteresis curve for all magnetite specimens is completely different from what we have seen for hematite (*cf.* Figs 2 and 6). For most magnetite specimens the remanent acquisition curve lies partially below the remanent hysteresis curve. The difference in relative position of the two curves is largest for the finest grain-size fractions.

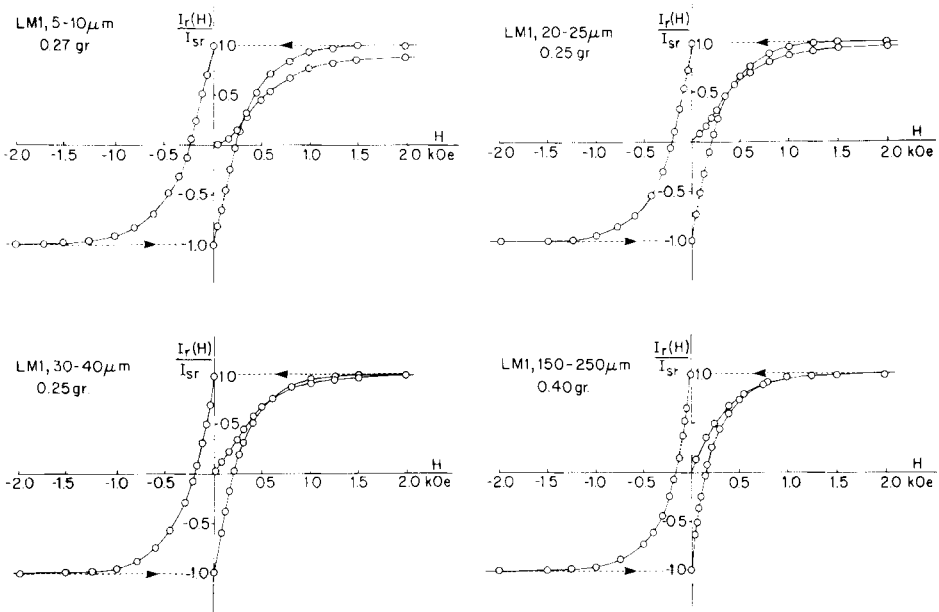


Figure 6. Normalized remanent acquisition curves and normalized remanent hysteresis curves of four different grain-size fractions of the same magnetite sample. The maximum direct magnetic field used was 20 kOe. In these diagrams only the part of the curves below 2 kOe is shown. The diagrams clearly show that the relative position of the remanent acquisition curve with respect to the remanent hysteresis curve changes with grain size. The difference between H'_{cr} and H_{cr} is largest for the finest grain-size fractions.

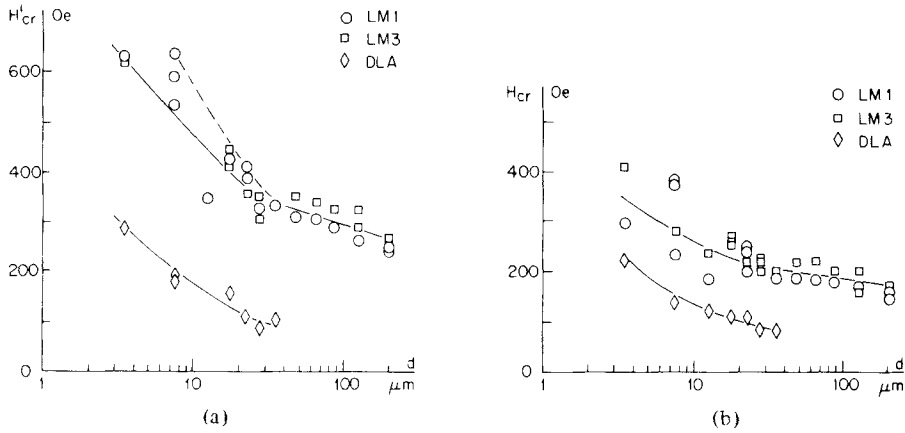


Figure 7. (a) Remanent acquisition coercive force (H'_{cr}) and (b) remanent coercive force (H_{cr}) for different grain-size fractions of magnetite samples LM 1 and LM 3, and titanomagnetite DLA.

As a consequence of the differences between the curves, the coercive forces derived from the curves, respectively H'_{cr} and H_{cr} are quite different. Both H'_{cr} and H_{cr} increase with decreasing grain size (Table 5, Fig. 7). H'_{cr} is larger than H_{cr} for each specimen and the difference between H'_{cr} and H_{cr} is largest for the finest grain sizes. H'_{cr} and, to a lesser extent, H_{cr} are dependent upon the quantity of magnetic material. A higher weight percentage and thus more closely packed grain assemblies of the same grain size reveal lower values of H'_{cr} and H_{cr} (Table 6). Similar observations were made by Day *et al.* (1977).

The diagrams which give the relation between H'_{cr} (H_{cr}) and grain size show a marked change in the slope for the magnetite data at about $30 \mu\text{m}$ (Fig. 7). This transition probably reflects a change in the domain configuration of magnetite from psd to md. Comparing the diagrams of Fig. 7 clearly shows that H'_{cr} has a higher resolution power to distinguish between psd and md grains than H_{cr} . The relationship between H'_{cr} and grain diameter is, however, also controlled by the quantity of magnetic material (Table 6, Fig. 7). If the relationship between H'_{cr} (H_{cr}) and grain diameter d can be approximated by the logarithmic function d_1^{-n} (d_1^{-m}) for grains smaller than $30 \mu\text{m}$ and by an expression d_2^{-n} (d_2^{-m}) for coarser grains (e.g. Stacey & Banerjee 1974, p. 66) then n_2 and m_2 are smaller than n_1 and m_1 respectively.

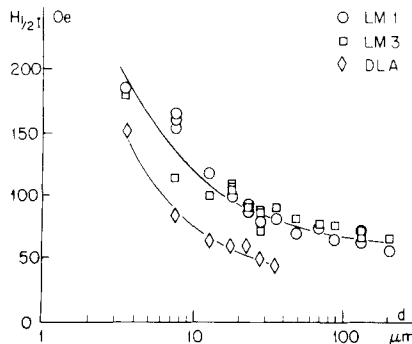


Figure 8. Median destructive field of the remanent saturation magnetization ($H_{1/2}$) for different grain-size fractions of magnetite samples LM 1 and LM 3 and titanomagnetite DLA.

For magnetite $n_1 = +0.27$ and $n_2 = +0.08$. Values for m_1 range from $+0.30$ to $+0.41$ and $m_2 = +0.12$. Titanomagnetite does not show a similar break in slope in the grain-size dependence, indicating that all grains have the same domain configuration which is supposedly to be psd. For titanomagnetite n_1 yields a value of 0.43 and $m_1 = 0.45$.

The median destructive field of I_{sr} , $H_{1/2I}$, depends also on the grain size but the values of $H_{1/2I}$ are much lower than for H'_{cr} and H_{cr} (Tables 5 and 6, Fig. 8). If $H_{1/2I} \propto d^{-1}$, then l_1 , for grain size finer than $30 \mu\text{m}$ is 0.40 and l_2 for larger grain sizes is 0.17 for magnetite. For most of the grain-size fractions from which specimens containing different quantities of magnetite were made, the specimens with the smallest amount of magnetite yielded the lowest $H_{1/2I}$. This trend is opposite to that of H'_{cr} for which the values tend to be higher for smaller amounts of magnetite.

$H_{1/2I}$ of titanomagnetite is lower than that of magnetite for all grain-size fractions. The value of l_1 for titanomagnetite is 0.53 .

Discussion

It is obvious that H'_{cr} , H_{cr} and $H_{1/2I}$ are not equal for magnetite and titanomagnetite specimens as they were for hematite specimens. H'_{cr} is larger than H_{cr} which in turn is larger than $H_{1/2I}$. The ratios between H'_{cr} and H_{cr} and between $H_{1/2I}$ and H_{cr} appear to be constant for all specimens of the same sample (Figs 9 and 10). Specimens of the same grain-size fraction but different weight percentages of magnetic material all have the same ratio. The ratios of H'_{cr}/H_{cr} for magnetite and titanomagnetite are respectively 1.6 ± 0.2 and 1.2 ± 0.2 , whereas values of $H_{1/2I}/H_{cr}$ are respectively 0.40 ± 0.06 and 0.59 ± 0.07 . The ratios for titanomagnetite are in between those for magnetite and hematite for both H'_{cr}/H_{cr} and

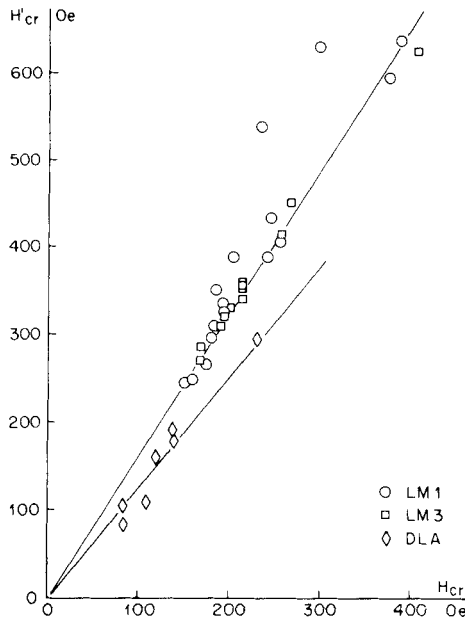


Figure 9. Relationship between the remanent acquisition coercive force (H'_{cr}) and the remanent coercive force (H_{cr}) for grain-size fractions of magnetite samples LM 1 and LM 3 and titanomagnetite DLA. For magnetite the ratio H'_{cr}/H_{cr} is 1.6 ± 0.2 and for titanomagnetite it is 1.2 ± 0.2 .

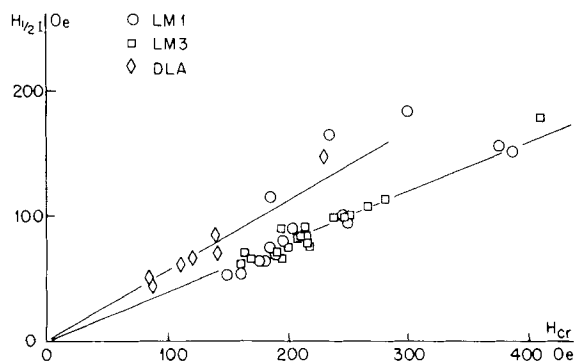


Figure 10. Relationship between the median destructive field of the remanent saturation magnetization ($H_{1/2I}$) and the remanent coercive force (H_{cr}) for grain-size fractions of magnetite samples LM 1 and LM 3 titanomagnetic DLA. For magnetite the ratio $H_{1/2I}/H_{cr}$ is 0.40 ± 0.06 and for titanomagnetite it is 0.59 ± 0.07 .

$H_{1/2I}/H_{cr}$. Probably H'_{cr}/H_{cr} increases with stronger spontaneous magnetization and $H_{1/2I}/H_{cr}$ decreases with it. The difference between H'_{cr} and H_{cr} is for each specimen about equal to the difference between H'_{cr} and $H_{1/2I}$. This gives a very simple relationship between the different parameters.

$$H'_{cr} - H_{cr} \approx H_{cr} - H_{1/2I}$$

or

$$H'_{cr} + H_{1/2I} \approx 2H_{cr}$$

This expression is independent of grain size and quantity of magnetic material in the range of 0.002 to 6 Vol per cent and is not only valid for magnetite and titanomagnetite but also for hematite where $H'_{cr} = H_{cr} = H_{1/2I}$.

Wohlfarth (1958) calculated that for an assembly of homogeneously distributed and randomly oriented non-interacting sd grains $H_{1/2I} \approx H'_{cr} \approx H_{cr}$. From his relations can be derived that if interaction takes place $H_{1/2I} < H_{cr} < H'_{cr}$. Dunlop & West (1969) modified Néel's (1955) theory by taking interaction between grains into account. They concluded that $H_{1/2I}$ is always lowered by interactions. Their observation that for elongated sd grains of synthetic magnetite $H_{1/2I} < H_{cr}$ (Dunlop & West 1969, fig. 8) was interpreted as being the result of interaction between grains. In Fig. 11 an attempt is made to visualize the effect of grain interaction on H'_{cr} , H_{cr} and $H_{1/2I}$. Assumptions made are that for an assembly of homogeneously distributed and randomly oriented grains, the interacting field between all grains is equal and has different orientations. There is a statistical net amount of grains having their magnetic moment in the direction of the remanent magnetization. The result of all interacting fields will then be oriented opposite to the direction of the remanent magnetization. For the acquisition of remanent magnetization it means that the interacting field H_i is opposite to the applied magnetizing field (Fig. 11a); so the effective magnetizing field is less than the applied field. Compared to a situation where no interaction occurs, a higher magnetizing field has to be applied to magnetize an interacting assembly of grains to one-half of its saturation magnetization. In other words, interaction between grains will cause an increase of the H'_{cr} . If an assembly of homogeneously distributed and randomly oriented grains which is magnetized to remanent saturation is remagnetized in a direction opposite to I_{sr} , the resultant interacting field will initially be in the same direction as the

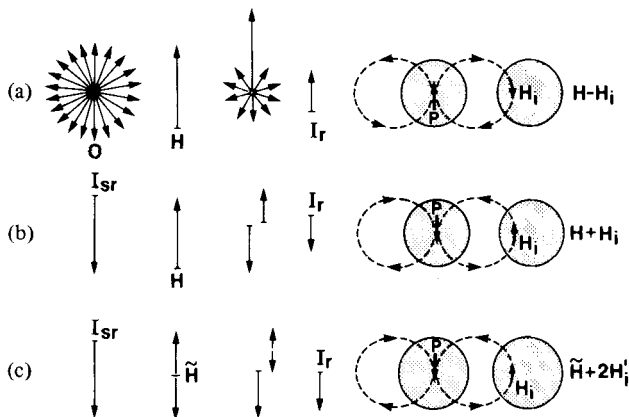


Figure 11. The effect of grain interaction upon coercivity parameters. (a) H_{cr} : if an unmagnetized assembly of magnetic grains is magnetized by a direct magnetic field H , the resulting magnetization I_r will be parallel to H . The interacting field H_i of one grain upon a neighbouring grain is opposite to H . The effective magnetizing field will therefore be $H - H_i$. Consequently H_{cr} for interacting grains must be greater than for non-interacting grains. (b) H_{cr} : if an assembly of magnetic grains having a saturation remanence I_{sr} , is being magnetized by a direct magnetic field H in a direction opposite to I_{sr} , the resulting magnetization I_r will at first be oriented opposite to H . The effective magnetizing field is then $H + H_i$. The effect of interaction on H_{cr} will be small because the strength of the interacting field decreases for decreasing I_r . (c) $H_{1/2I}$: if an assembly of magnetic grains having a saturation remanence I_{sr} is being demagnetized with alternating magnetic field \tilde{H} , the unblocked magnetic moments are aligned opposite to each other. The unblocked magnetic moments cause oppositely oriented interacting fields H_i which are parallel to the two branches of \tilde{H} . The effective demagnetizing field will therefore be $\tilde{H} + 2H_i$, which means that $H_{1/2I}$ for interacting grain assemblies is smaller than for non-interacting grain assemblies. The effect of interaction will be largest for high demagnetizing fields. The effective demagnetizing field will be asymmetrical because I_r also causes an interacting field.

magnetizing direct field so that the effective remagnetizing field is higher than the applied field (Fig. 11b). The H_{cr} will therefore be reduced by interaction. Alternating field demagnetization of I_{sr} gives opposite orientation of equal amounts of unblocked magnetic moments. Interacting fields between unblocked magnetic moments are parallel to the branches of the applied alternating field and therefore cause an increase of the effective demagnetizing field and reduction of $H_{1/2I}$ (Fig. 11c). Because the remanent magnetization and related interaction is only parallel to one of the branches of the alternating field, it is possible that due to interaction, the effective demagnetizing field becomes asymmetrical.

Summarizing, it can be said that due to interaction H'_{cr} will increase, H_{cr} will slightly decrease and $H_{1/2I}$ will decrease significantly. The ratio H'_{cr}/H_{cr} must therefore be larger than 1 if interaction between grains occurs and the ratio $H_{1/2I}/H_{cr}$ smaller than 1. The stronger the interaction is, the larger the deviation of the ratios from 1. If the results for hematite, magnetite and titanomagnetite specimens are compared, it is obvious that no interaction exists for hematite grains and that magnetite exhibits the strongest interaction. The ratios H'_{cr}/H_{cr} and $H_{1/2I}/H_{cr}$ appear to be the same for all grain sizes and also for different quantities of one grain size. The decrease of H'_{cr} and increase of $H_{1/2I}$ for increasing quantity of magnetite of the same grain size (Table 6) cannot be explained by interaction, since higher packing density leading to stronger interaction should theoretically produce higher H'_{cr} and smaller $H_{1/2I}$. This is completely opposite to the changes observed upon increasing the packing density, which means that the relation between H'_{cr} , H_{cr} and $H_{1/2I}$ is not entirely determined by interactions.

Conclusions

For assemblies of homogeneously distributed and randomly oriented non-interacting hematite grains between 250 and 5 μm , H'_{cr} , H_{cr} and $H_{1/2\text{I}}$ all vary with grain size but are nearly equal for the same specimen. The difference between md grains and psd grains of hematite is reflected by an abrupt change in the slope of the coercivity curves versus grain size. Assemblies of homogeneously distributed and randomly oriented magnetite grains ranging in size between 250 and 5 μm and in volume percentage from 5 to 0.002 have an H'_{cr} which is larger than H_{cr} and an $H_{1/2\text{I}}$ which is smaller than H_{cr} . The difference between H'_{cr} and H_{cr} as well as between H_{cr} and $H_{1/2\text{I}}$ is largest for the finest grain-size fractions, having the highest M_{sr} . Higher packing density of the same grain-size fraction of magnetite appears to result in a decrease of H'_{cr} , an effect which is opposite to that expected from a theoretical point of view if only interaction is taken into account. The ratios $H'_{\text{cr}}/H_{\text{cr}}$ and $H_{1/2\text{I}}/H_{\text{cr}}$ appear to have a (different) constant value for the same type of magnetic mineral irrespective of grain size or packing density. For hematite both ratios are close to 1. For magnetite $H'_{\text{cr}}/H_{\text{cr}}$ is larger than 1 whereas $H_{1/2\text{I}}/H_{\text{cr}}$ is smaller than 1. Values for titanomagnetite are in between those for magnetite and hematite for both ratios. For all specimens containing homogeneously distributed and randomly oriented grains of magnetite, titanomagnetite or hematite, the relation between the different coercivities is close to $H'_{\text{cr}} + H_{1/2\text{I}} \approx 2H_{\text{cr}}$.

Acknowledgments

The measurements for this study were made as a part of a PhD thesis under the supervision of J. D. A. Zijderveld of the Paleomagnetic Laboratory of the State University of Utrecht. His stimulating discussions and critical remarks are gratefully acknowledged. I would like to thank P. J. Verplak and H. J. Meijer for the magnetic measurements and R. P. E. Poorter for the microprobe analysis. I am also indebted to J. L. Roy and W. A. Morris for reading and improving the manuscript.

References

- Dankers, P. H. M., 1978. Magnetic properties of dispersed natural iron-oxides of known grain-size, *thesis*, State University of Utrecht, 142 pp.
- Davis, P. M. & Evans, M. E., 1976. Interacting single-domain properties of magnetite intergrowths, *J. geophys. Res.*, **81**, 989–994.
- Day, R., Fuller, M. D. & Schmidt, V. A., 1977. Hysteresis properties of titanomagnetites: grain-size and compositional dependence, *Phys. Earth planet. Int.*, **13**, 260–267.
- Dunlop, D. J. & West, G. F., 1969. An experimental evaluation of single domain theories, *Rev. Geophys.*, **7**, 709–757.
- Green, G. M. & Cornitius, L. E., 1971. A technique for magnetically separating minerals in a liquid mode, *J. sedim. Petrol.*, **41**, 310–312.
- IJlst, L., 1973. A laboratory overflow-centrifuge for heavy liquid mineral separation, *Am. Miner.*, **58**, 1088–1093.
- Levi, S. & Merrill, R. T., 1978. Properties of single-domain, pseudo-single-domain and multidomain magnetite, *J. geophys. Res.*, **83**, 309–323.
- Néel, L., 1955. Some theoretical aspects of rock magnetism, *Phil. Mag. Suppl.*, **4**, 191–242.
- Parry, L. G., 1965. Magnetic properties of dispersed magnetite powder, *Phil. Mag.*, **11**, 303–313.
- Stacey, F. D. & Banerjee, S. K., 1974. *The Physical Principles of Rock Magnetism*, Elsevier, Amsterdam, 195 pp.
- Wohlfarth, E. P., 1958. Relations between different modes of acquisition of the remanent magnetization of ferromagnetic particles, *J. Appl. Phys.*, **29**, 595–596.